Industrial Crops and Products 96 (2017) 149–157

Contents lists available at ScienceDirect

Industrial Crops and Products

journal homepage: www.elsevier.com/locate/indcrop

Research Paper

Distribution and penetration of tung oil in wood studied by magnetic resonance microscopy

Mojca Žlahtič[a], Urška Mikac[b], Igor Serša[b], Maks Merela[a], Miha Humar[a,*]

[a] University of Ljubljana, Biotechnical Faculty, Dept. of Wood Science and Technology, Jamnikarjeva 101, SI-1000, Ljubljana, Slovenia
[b] Jožef Stefan Institute, Jamova 39, SI-1000, Ljubljana, Slovenia

ARTICLE INFO

Article history:
Received 12 September 2016
Received in revised form
23 November 2016
Accepted 24 November 2016

Keywords:
Tung oil
Wood protection
Magnetic resonance imaging
MRI
Wood

ABSTRACT

Water repellents, as environmentally-friendly treatments, are gaining popularity as non-biocidal solutions for wood protection. Drying oils, in addition to waxes and organosilicon compounds, are one of the most important water repellents for wood. Tung oil has so far been proven to be one of the best performing oils for wood protection. However, tung oil, similarly as other oils, does not penetrate deeply into wood, due to its high viscosity. In order to improve the penetration of oil into wood, a vacuum-pressure procedure has to be applied. The species used in this study are important in Central Europe: sweet chestnut heartwood (*Castanea sativa*), European larch heartwood (*Larix decidua*), Scots pine heartwood and sapwood (*Pinus sylvestris*) and Norway spruce (*Picea abies*). Oil uptake depends on the applied impregnation method and on the wood species used. Retention of tung oil was higher after an impregnation process than with the immersion procedure. Magnetic resonance imaging (MRI) was applied to elucidate the influence of wood species on oil penetration and distribution in wood after treatment. High spatial resolution MR imaging is highly sensitive to changes of liquids in wood and is therefore also very appropriate for monitoring oil penetration. Furthermore, with a good signal to noise ratio of MR images, the method can also discern among specimens with different patterns of oil distribution, as well as between areas of early-wood and late-wood.

1. Introduction

Increased environmental concerns in recent years have resulted in renewed interest in non-biocidal solutions for wood preservation. These techniques include proper selection of wood species, wood modification, proper planning of construction details and the application of various hydrophobic treatments (Palanti et al., 2011; Thybring, 2013). Their mode of action is based on reducing the rate of water uptake into the capillaries. These hydrophobic treatments usually only slow down water penetration without fully preventing it, so they are not meant to be used where there is ground contact. If the wood moisture content is kept low enough, fungal decay is no longer possible (Goethals and Stevens, 1994; Lesar and Humar, 2010). After a long period of soaking in water, wood treated with water repellents usually retains similar amounts of water and swells to the same extent as untreated wood (Thybring, 2013). However, most wood in use of class 2 (above ground, covered) and class 3 (above ground, uncovered) EN (2013) is exposed to weathering for limited periods only, hence water repellents perform well in such conditions. One of the most important requirements for water repellents applied outdoors is that they should not seal the surface of the wood. A surface film makes water diffusion possible, which enables drying of the wood after precipitation (Williams and Feist, 1999). One of the most important water repellents used in wood preservation other than waxes (wax emulsions) (Lesar and Humar, 2011) and organosilicon compounds (De Vetter et al., 2009) is drying oils (Schultz et al., 2007). Tung oil is a drying oil obtained by pressing seeds from the nut of the tung tree (*Vernicia fordii; V. montana*). As a drying oil, tung oil dries when exposed to air, forming a transparent film. Tung oils consist of the following fatty acids: palmitic acid (5.5%), oleic acid (4.0%), linoleic acid (8.5%) and alpha-eleostearic acid (82.0%) (Anon, 2016). Its water-repellent efficacy has been proven in several laboratory and field trials (Humar and Lesar, 2013). We have proven its excellent water repellence even after severe aging and weathering procedures (Žlahtič and Humar, 2016). Data from these studies clearly show that the performance of drying oils depends on the amount of applied oil, i.e., treatment procedures. As reported for several other preservative systems, penetration and retention do not depend on the treatment procedure only but also on the wood species used (Banks, 1970; Siau, 1984; Kumar and Morrell, 1989). Refractory wood species are rarely used for wood impregnation procedures, since target retention and

* Corresponding author.
E-mail address: miha.humar@bf.uni-lj.si (M. Humar).

http://dx.doi.org/10.1016/j.indcrop.2016.11.049
0926-6690/

penetration is difficult to achieve. Permeability is influenced by a variety of factors, including sapwood-heartwood ratio, density, presence of bordered pits, tyloses, size of vessels and tracheids and pits and resin canals, as well as pre-treatment such as drying or hydrothermal treatment of wood (Flynn, 1995; Durmaz et al., 2015). It can be presumed, that the importance of the natural products isolated from various industrial crops will increase in the developed countries, as end users are avoiding the toxic biocides, and are using alternatives of natural origin instead. Even more, these alternatives have to be produced with industrial techniques with the lowest environmental impact.

There are different pathways how water moves through the wood. In dried wood, during impregnation liquids takes various pathways (Zimmer et al., 2014). In axial direction impregnation solution moves through the tracheids (conifers) or vessels (hardwoods), that are connected with pits. At conifers bordered pits connects the tracheids. However, the anatomical assembly of bordered pits permits the maintenance of a xylary water column, while preventing the spread of air through embolized tracheids (Maschek et al., 2013). This mechanisms enables survival of the trees but on the other hand causes problems during impregnation. Hence, the number, size and aspiration state of the bordered pits greatly influence the treatability of coniferous sapwood (Stamm, 1947; Militz, 1993; Zimmer et al., 2014). Small diameter latewood tracheids as well as the portion of unaspirated pits in the latewood fraction positively influence treatability (Sedighi-Gilani et al., 2012). On the other hand it should be considered, that axial planes in the wood are limited, thus flow of the preservative solutions in radial and tangential direction is even more important. In radial direction, fluid transport occurs through the rays. For example, in Scots pine, the ray system consist of ray tracheids and ray parenchyma (Wagenführ, 1996).

This paper elucidates the influence of wood species and treatment method on tung oil retention and permeability of selected wood species. Permeability is a key wood parameter important for impregnation or drying processes. The magnetic resonance imaging (MRI) method was used to analyse oil uptake *in situ*. MRI is a non-destructive, non-invasive and non-contact technique already being successfully applied in wood science (Bucur, 2003a, 2003b; Merela et al., 2005; Oven et al., 2011) and with other porous materials (Moreaux and Dereppe, 1994; Demeure et al., 1994). Wood is an ideal material for MRI studies, due to its high moisture content when green and its hygroscopic character when in use (Oven et al., 2011). In the case of dry wood, as for example in our study, the moisture content of wood was kept so low that there was no free water and only tung oil can be seen on the MR images due to the protons in a liquid state inside the oil. The prime objective of this study was to determine the suitability of the method of MRI, and to prove the influence of wood species and treatment method on tung oil retention, penetration and distribution. The aim of this study was to employ the 3D MRM technique to visualize the oil distribution and penetration in various wood species and to make a correlation between oil retention and the MRI signal. This method was used because, in addition to the total amount of oil, it can also detect the spatial oil distribution in the wood sample. MRM refers to very high resolution MRI imaging, with resolution down to nanometre scale. Resolution of the classical MRI is typically about one mm^3.

2. Materials and methods

2.1. Material

The present study was performed on economical important wood species in Central Europe that are frequently used in class 2 and 3 applications. In order to improve their outdoor performance, they are frequently treated with various oils, like linseed and tung oil. The magnetic resonance imaging (MRI) method was used to analyse oil uptake in situ. The following materials were utilised: chestnut heartwood (*Castanea sativa*), European larch heartwood (*Larix decidua*), Scots pine heartwood and sapwood (*Pinus sylvestris*) and Norway spruce (*Picea abies*) wood. Specimens were defect-free, without visible signs of decay or blue staining, as prescribed in standard EN (2006). The materials were classified into various treatability classes as prescribed in standard EN (2015). Sweet chestnut heartwood (class 4), spruce heartwood (class 3-4), larch heartwood (class 4) and scots pine heartwood (class 3-4) belong to the group of the wood species that are extremely difficult to treat. Only scots pine sapwood has been classified as an easily treated material (class 1). This selection of the materials offers us observation of the oil penetration to wood species with various anatomical characteristic (softwoods vs hardwoods; sapwood vs heartwood; permeable vs impermeable; ring porous wood).

The dimensions of the samples used for tensiometer experiments were 5.0 cm × 1.5 cm × 2.5 cm (longitudinal × radial × tangential). The dimensions of the specimens used for MRM scanning were initially 7 cm × 1.2 cm × 1.2 cm (longitudinal × radial × tangential). These specimens were treated with tung oil (Samson, Kamnik, Slovenia) and then sawn into five smaller specimens, as indicated on Fig. 1. The dimensions of the specimens used in the MRM study were limited by the size of the RF coil.

Selected samples were treated with tung oil (Humar and Lesar, 2013) to improve the hydrophobic properties of the wood. Half of the specimens used for MR imaging were impregnated with oil and the other half were immersed in oil for 1 min. Impregnation was performed according to the full cell process, i.e., 30 min vacuum (80 mbar), 120 min pressure (8 bar), 15 min vacuum (80 mbar) and 20 min soaking. The remains after both treatments were wiped off with paper towel. Uptake of the oil was determined gravimetrically. It is believed that after drying slightly lower amount of oils remained in the wood because of volatile compounds that afterwards evaporate from the wood. After impregnation, samples were dried for 4 weeks at room temperature (20 °C; RH = 60%).

2.2. Uptake of tung oil and water on tensiometer

The longitudinal direction is the most prominent pathway for liquid penetration; it was therefore elucidated with tensiometer analysis. The cross section surfaces of the specimens were exposed to oil for 200 s, to determine tung oil uptake in the longitudinal direction. The measurements were carried out at room temperature (≅20 °C) and RH of 60 ± 5% on a Tensiometer K100MK2 device (Krüss, Germany) according to a modified EN 1609 standard (1997). Specimens were positioned so that the wood cross section surface was in contact with the test liquid and their masses were subsequently measured continuously every 2 s for 200 s. The velocity before contact was 6 mm/min, the sensitivity of contact was 0.005 g and the depth of immersion was set at 1 mm. Depending on the final weight and cross section surface of the immersed sample, the uptakes of tung oil in grams per square centimetre were calculated. For comparison, samples were also immersed in water according to the same procedure.

2.3. High-resolution magnetic resonance imaging

MRM experiments were performed on a TecMag Redstone (USA) MRI spectrometer with a superconducting 9.4 T magnet (Jastec, Japan). The specimens were imaged in a 20-mm diameter RF coil. To obtain the oil distribution along the longitudinal, tangential and radial directions, 1D MRM was used with the following parameters: field of view (FOV) of 20 mm, echo time (TE) of 1.6 ms, repetition

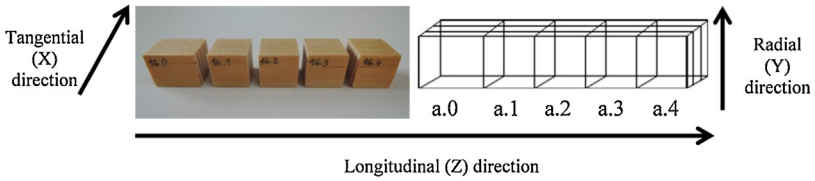

Fig. 1. Specimens prepared for magnetic resonance imaging.

time (TR) of 1 s and resolution of 156 μm. In order to visualize the 3D distribution of the oil, the 3D MRM was performed by a gradient-echo technique with the following parameters: FOV of 20 mm, imaging matrix 128 × 128 × 128 (isotropic resolution was 156 μm), excitation flip angle 19°, TE of 1.1 ms, TR of 50 ms and total imaging time of 34 min. For selected samples, MR images with higher spatial resolution (imaging matrix 256 × 256 × 256 (isotropic resolution was 78 μm) leading to total imaging time of 7.5 h) were also performed.

The 1D MRM datasets were analysed by ImageJ (National Institute of Health, USA) digital image processing software. The settings for the MRM measurements were not the same for different samples (probe tuning, receiver gain. . .); normalization of the 1D MRM signals was therefore performed in an axial (Z) direction. The signals from one wood specimen (5 samples sawn from the original one) were first normalized so that the signal values at the edges at which the original sample was sawn were the same. For normalization between samples from different wood species, the sum of the signals from all 5 samples was compared with tung oil retention. The ratio between the total signal and the oil mass was then normalized to the same ratio of the pine sapwood (impregnated). The impregnated pine sapwood sample was chosen because of its highest signal intensity and mass increase after treatment.

3. Results and discussion

3.1. Uptakes of oil

The average uptake of tung oil with different wood specimens, applied with two different treatment procedures, is shown in Table 1. These data clearly show the influence of wood permeability on the effectiveness of the treatment procedure. The treatments had different effects on the retention of tung oil. As expected, vacuum-pressure impregnation resulted in higher uptakes of oil than the immersing procedure (Table 1).

The highest retention was determined with vacuum-pressure treated pine sapwood (413.7 kg/m^3), which was approximately 20 times higher than that achieved by the immersion procedure (20.4 kg/m^3). The difference among procedures was more pronounced with more permeable species than with refractory ones. The data on uptakes of oil in wood are in line with treatment data reported in the standard. The highest uptakes determined with pine sapwood (413.7 kg/m^3) were roughly six times higher than those determined with pine heartwood (65.9 kg/m^3). The discrepancy can be explained by the permeability of pine sapwood, which is considerably greater (approximately 10 times) than that of heartwood (Siau, 1984; EN, 2015). It was rather surprising that higher uptakes of oil after vacuum-pressure impregnation were determined with refractory spruce (119.3 kg/m^3) than with pine (65.9 kg/m^3) and larch heartwood (39.0 kg/m^3); the latter two species belong to the same group of refractory wood species. The second highest uptake after vacuum pressure impregnation was determined with sweet chestnut wood (186.6 kg/m^3), presumably due to the large pore diameters. This presumption is due to be confirmed with MRI studies. The lowest oil uptake was determined with immersed larch wood (3.4 kg/m^3). This clearly shows the refractory nature of this wood species. Similarly, as reported for the vacuum-pressure procedure, the highest uptake after immersion was also found with pine sapwood (20.4 kg/m^3).

Observations in tensiometer uptakes differ from determined uptakes. A tensiometer provides information on the dynamic of oil penetration in wood. The permeability of highly anisotropic wood varies with structural direction. Ratios of longitudinal to transverse permeability as high as 10^6 have been observed in some species (Comstock, 1970). The highest uptake of oil was determined with spruce (0.18 g/cm^2) and the lowest with larch (0.06 g/cm^2) (Table 1). The uptake of oil to pine sapwood (0.12 g/cm^2) and heartwood (0.10 g/cm^2) was comparable, while the penetration of oil to sweet chestnut was between larch and pine heartwood (0.08 g/cm^2). As expected, there was no correlation between tensiometer uptake and vacuum-pressure uptake; however, it was rather surprising that tensiometer uptake and immersed uptake were also not related. The only correlation was that the lowest oil uptake was determined with larch wood by tensiometer, after the immersion and vacuum pressure procedure (Table 1). The reasons for this phenomenon may be associated with the fact that the ratio of cross section planes of the specimens is fairly low; it does not therefore have a prevailing influence on the oil uptake. The liquid in axial directions moves predominately through the tube system made of axial tracheids (softwods) and trachea (ring porous hardwoods), which are interconnected by bordered pits (softwoods) or perforations (hardwoods). In contrary, there are considerably less tissues in wood that enables liquid penetration in radial or tangential direction available, with exemption of ray parenchyma (Wagenführ, 1996; Zimmer et al., 2014). Comparing those results to the average water uptake, the highest uptake was determined with pine sapwood (0.21 g/cm^2) and the lowest with larch (0.05 g/cm^2) (Table 1). The water uptake was similar to tung oil uptake with pine heartwood, larch and chestnut. Bigger differences were determined with pine sapwood, with which water uptake was 0.21 g/cm^2 and tung oil uptake was almost half of that. Longitudinal penetration of liquids into wood is a fairly complex phenomenon. It is influenced by density and other anatomical factors that influence permeability (Larnøy et al., 2008; Lande et al., 2010; Zimmer et al., 2014). The key factors are size and frequency of parenchyma rays, half-bordered pits between parenchyma rays and tracheids (fenestriform pits), aspiration of bordered pit pairs of tracheids, ratio of earlywood/latewood, amount and constitution of heartwood, presence and characteristics of resins in the sapwood, presence of tyloses (with chestnut) and other structural features. It was shown for the Scots pine, that frequency of both radial and axial resin canals does not significantly influence the permeability. However, the differences in treatability could consequently also be a result of different proportions of lignified parenchyma cell walls due to aging processes of samples with different annual ring widths (Zimmer et al., 2014).

3.2. Magnetic resonance imaging

Figs. 2–5 present plots, showing the signal intensity in all three directions, longitudinal (Fig. 2), tangential (Figs. 3–5) and radial (Figs. 3–5). Since the specimen was too big for analysis due to the

Table 1
Average uptakes of tung oil and water. Standard deviations are provided in parenthesis.

Wood Specimens	Scientific Name	Abbrev.*	Treatability class**	Treatment procedure and uptake of tung oil (kg/m^3)		Average tung oil uptakes in tensiometer (g/cm^2)	Average water uptakes in tensiometer (g/cm^2)
Scots Pine (Sapwood)	*Pinus sylvestris*	*PsS*	1	Impregnation	413.7 (47.1)	0.12 (0.012)	0.21 (0.054)
				Immersing	20.4 (1.9)		
Scots Pine (Heartwood)	*Pinus sylvestris*	*PsH*	3-4	Impregnation	65.9 (3.7)	0.10 (0.023)	0.10 (0.011)
				Immersing	7.7 (0.5)		
European Larch	*Larix decidua*	*Ld*	4	Impregnation	39.0 (1.2)	0.06 (0.004)	0.05 (0.014)
				Immersing	3.4 (0.4)		
Sweet Chestnut	*Castanea sativa*	*Cs*	4	Impregnation	186.6 (13.4)	0.08 (0.008)	0.10 (0.011)
				Immersing	8.3 (0.5)		
Norway Spruce	*Picea abies*	*Pa*	3-4	Impregnation	119.3 (7.3)	0.18 (0.01)	0.12 (0.069)
				Immersing	9.1 (0.6)		

*The materials abbreviations are used later in plots.
**EN (2015).

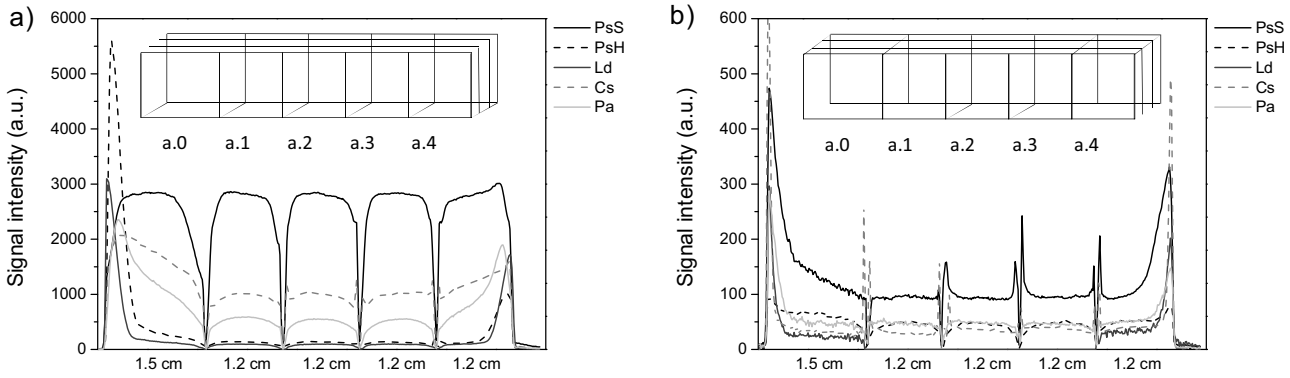

Fig. 2. Intensity of the MR signal of tung oil in wood species after vacuum-pressure impregnation (a) and after immersion (b) in a longitudinal direction (Z) with four different wood species. The materials abbreviations are the same as in Table 1.

small size of the RF coil, it was additionally cut into smaller pieces (Fig. 1). If a smaller specimen, which would fit into the MRI instrument, were to be used for impregnation, the edge effect would be too prominent.

On the first plot (Fig. 2a), specimens from a.0 to a.4 are arranged on the *x*-axis. Specimen a.0 and a.4 originate from the edges of the original specimen, while a.1, a.2 and a.3 are the central ones (longitudinal direction). Spaces between peaks in Fig. 2 indicate parts that were lost during cutting. From the profiles in Fig. 2, the retention level can mostly be seen, depending on impregnation (a) or immersion (b) in the longitudinal direction. Regardless of the treatment procedure, a higher signal can be seen at the far right (a.0) and far left side (a.4) of the specimen (profile). The signal intensity is proportional to the amount of tung oil. The peaks in the signal profiles can be attributed to better tung oil penetration in the longitudinal direction. A more uniform signal is observed in wood specimens with higher permeability, whereby the oil penetrated through the entire surface more uniformly. The best example of this is vacuum-pressure impregnated Scots pine sapwood. All five cut samples have a similar signal intensity, around 2800 a.u. (arbitrary units that reflects normalised signal intensity), without significant deviations. In the tangential direction, Fig. 5(a and b), the signal is much more uniform than in the longitudinal direction (Fig. 2), on radial spectra (Fig. 5c and d), peaks representing late- and early-wood areas can be clearly seen.

Fig. 2 shows a comparison between two treatment procedures. After impregnation, the scale on the y-axis (in the longitudinal direction) reached up to 6000 a.u., while immersion resulted in almost 10 times lower values, which is in line with gravimetric studies. In radial and tangential directions, the signal was lower but the ratio between the signals from impregnated and immersed specimens remained the same (Fig. 5). The maximum MRI signal obtained with pine treated by immersion in the longitudinal direction was around 470 a.u. Immersion of the samples in oil resulted in lower MRI signals compared to the vacuum-pressure treated samples, which is in line with gravimetrically determined retention (Table 1). Since the oil did not penetrate into the wood, there are more prominent differences noted between the edges and central parts of specimens. During immersion the predominant path for penetration is the longitudinal direction. Both edge parts had a signal intensity between 330 a.u. and 470 a.u., while the signal intensity of the central part was approximately 100 a.u. In addition to peaks at the edges of the specimens in the longitudinal direction, there are some local maxima resolved in the central parts of the specimens, which can be predominantly seen with immersed specimens or with specimens in which lower uptake was observed (Table 1). For example, this can be seen with pine heartwood, chestnut and larch (Fig. 2a and b). We presume that the reason for these phenomena originates in the subsequent sawing, whereby some of the tung oil smudged across the surface with the saw blade. This can be explained as a methodological defect.

Distributions of oil in pine heartwood (Fig. 2) had a considerably lower signal intensity, which can be explained by lower retention due to the refractory nature of heartwood in comparison to sapwood specimens. Heartwood formation processes resulted in differences between sapwood and heartwood permeability. Immersion of pine heartwood in oil resulted in almost 10 times lower oil retention (Table 1) than with impregnation. However, both vacuum-pressure processes, as well as immersion, resulted in a predominantly surface accumulation of tung oil. A smaller amount of oil also penetrated in early-wood vessels. With oil impregnated specimens from the central part (a.1, a.2 and a.3), the MRI signal intensity was around 130 a.u. in the longitudinal direction (Fig. 2). This is comparable to the value for specimens

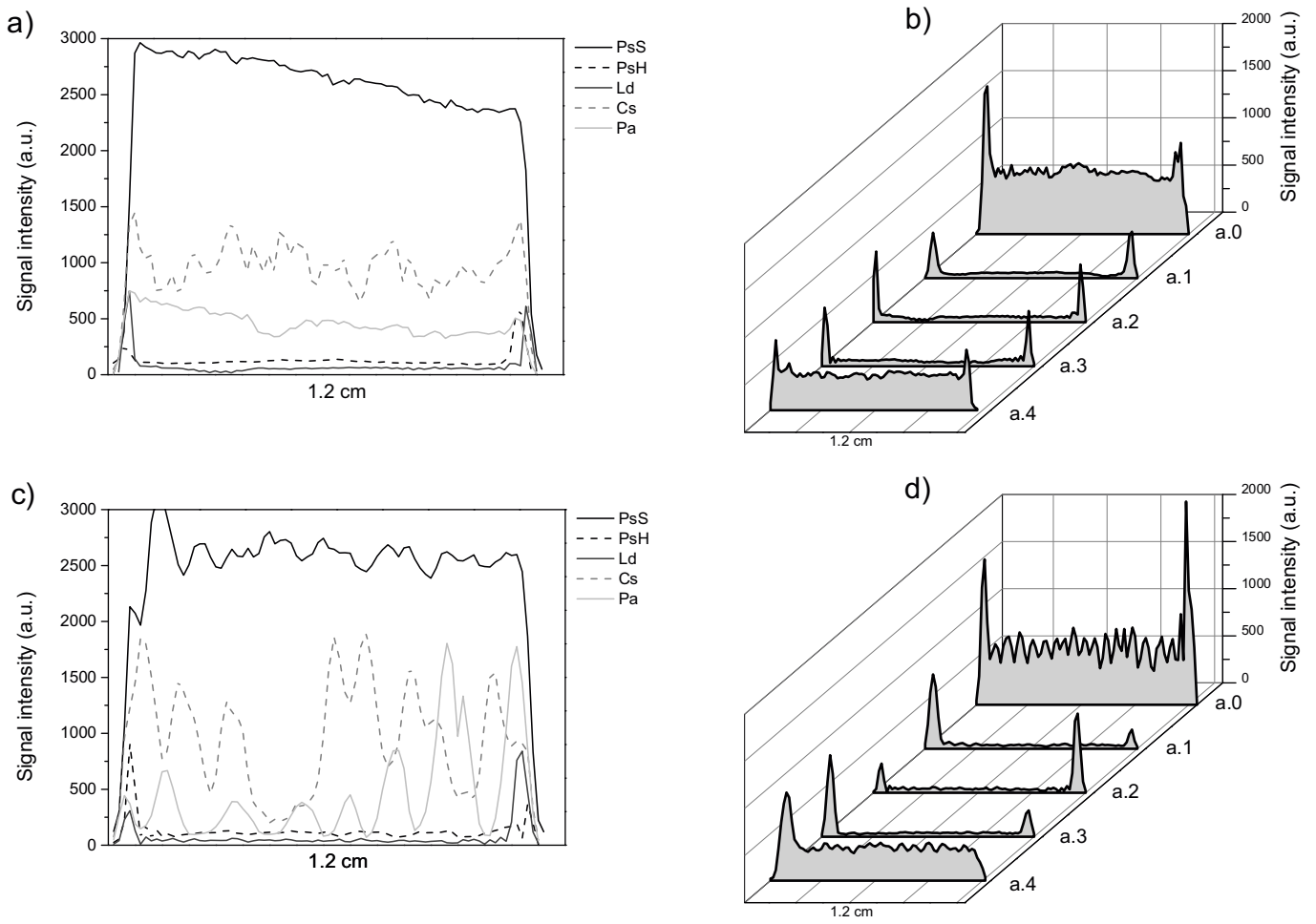

Fig. 3. Influence of various wood species on the intensity of the MR signals of tung oil in wood species after vacuum-pressure impregnation in a tangential (X) direction (a) and a radial (Y) direction (c) for central (a.2) specimens only. In 3D plots (b, d) all five specimens in tangential (b) and radial (d) directions for Larch samples (Ld) can be seen. The materials abbreviations are the same as in Table 1.

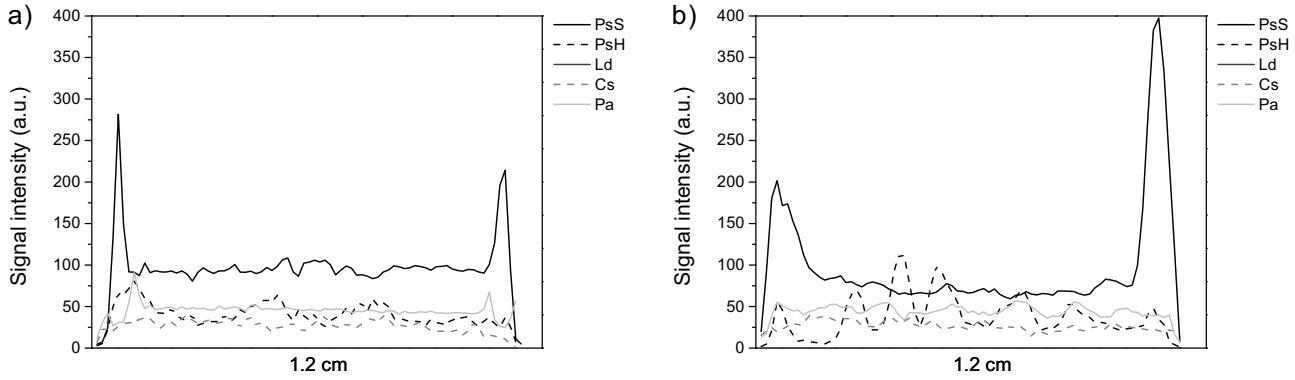

Fig. 4. Intensity of the MR signals of tung oil in wood species after immersing in a tangential (X) direction (a) and in a radial (Y) direction (b) for a.2 specimens (Fig. 1). The materials abbreviations are the same as in Table 1.

that were immersed only (50 a.u.). Similar values clearly indicate that the oil did not penetrate into the pine heartwood specimens in radial and tangential directions, even after a vacuum-pressure procedure. On the other hand, the intensity of the MRI signal at the edges of the impregnated specimens was much higher. Namely, an intensity of 5500 a.u. was determined on one side and 1000 a.u. on the other side, which reflects good penetration in the longitudinal direction. Immersion resulted in lower uptakes in the longitudinal direction, which was expected. However, as reported for the gravimetrically determined uptake data, tensiometer results does not fully correlates to MRI measurements. It can be presumed, that the prime reason for this fact is, that tenziometer data reflects the penetration in axial direction, while MRI and gravimetric assay reveal the uptakes in all of the directions.

As reported for gravimetrically determined uptakes, the lowest signals of tung oil were determined with larch wood. The 3D plots in Fig. 3b and d shows the distribution of tung oil in each larch specimen in tangential and radial directions. In the radial direction

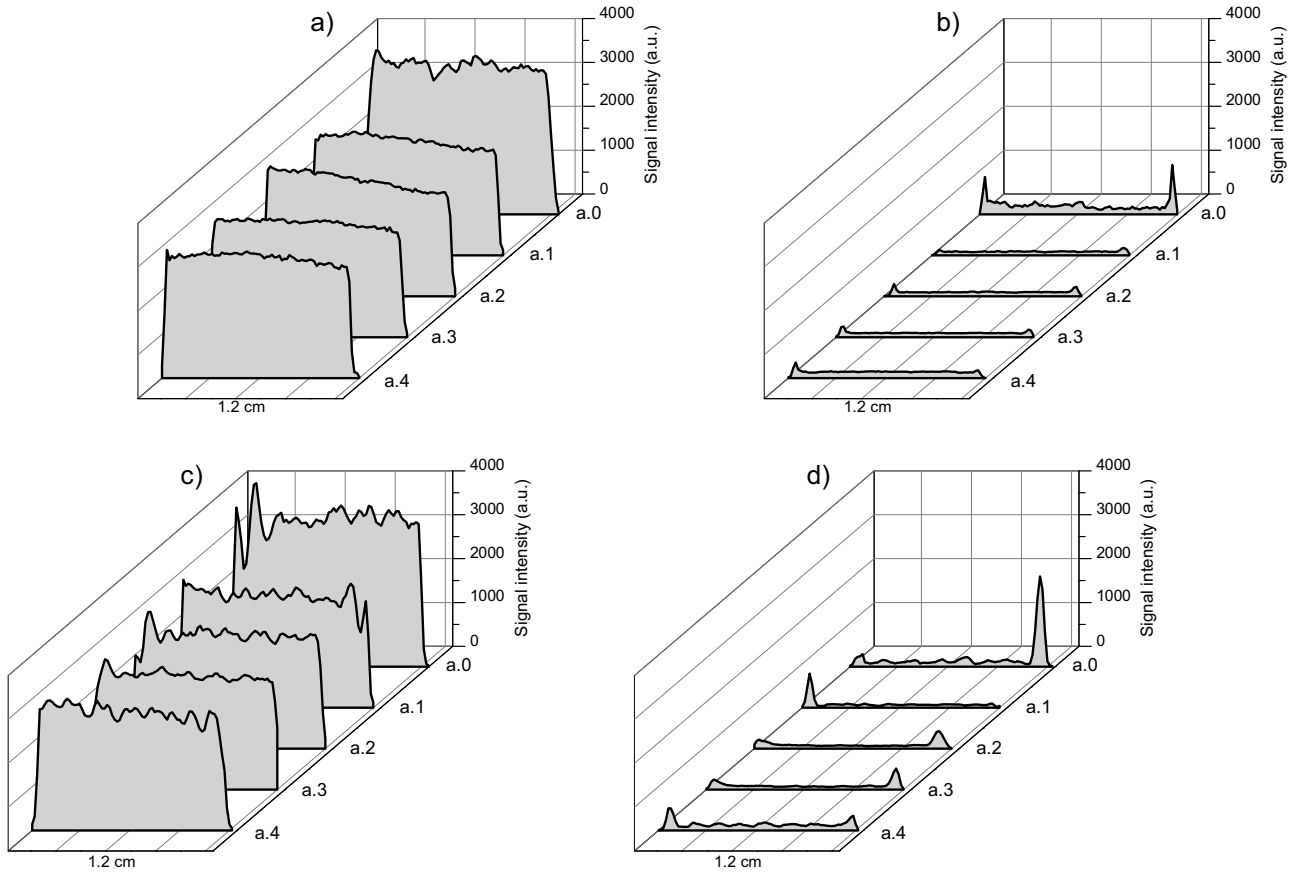

Fig. 5. Intensity of the MR signals of tung oil in Scots pine sapwood after vacuum-pressure impregnation (a,c) and after immersion (b,d) in a tangential (X) direction (a,b) and a radial (Y) direction (c,d). In 3D plots all five specimens of PsS can be seen.

(Fig. 3d), growth rings can also be detected, due to proper orientation and uniform growth (because of the wood structure, early wood contained more oil and had a higher MR signal). Similarly, as already reported, higher signals at the edges were determined (Figs. 2 and 3). After vacuum-pressure impregnation, the signal from central specimens in a longitudinal direction (Fig. 2) was around 100 a.u. and between 1700 a.u. and 3090 a.u. at the edges. After brushing, hardly any signals were determined for the inner specimens, which clearly demonstrates the refractory nature of larch heartwood. Similarly, as reported for pine heartwood, a higher oil content was determined at the edges.

Spruce is one of the most important European wood species that is widely used for construction and other outdoor applications. This wood species is refractory and thus challenging to impregnate. Similarly as reported for pine wood, higher oil retention was determined after impregnation than with immersion (Fig. 2). Retention of oil after impregnation determined with MRI (550 a.u.) was lower than for pine sapwood (2800 a.u.) and chestnut (1000 a.u.) but higher than for pine heartwood (140 a.u.) and larch (100 a.u.). At the edges, maximum values between 1900 a.u. and 2300 a.u. were determined. The distribution of oil in vacuum-pressure treated spruce was similar to the distribution of oil in pine heartwood. However, in the lower set of the MRI images, a variation in spruce wood can be observed (Fig. 6c). The majority of tung oil penetrated into the lower two growth rings. This could also indicate that the specimen was not only of heartwood but highly impregnated growth rings belonged to sapwood. In sweet chestnut, as a ring-porous wood (Fig. 6a), the majority of tung oil penetrated to the early-wood vessels (specimens were made of heartwood only). We were rather surprised that oil penetrated through the whole cross-section of impregnated specimens (uniform signal on Fig. 2). Differences between central specimens and the outer ones were lower than with refractory spruce and larch. This indicates that the vessels represent an important pathway for oil penetration. On closer inspection of Fig. 3, several smaller peaks in tangential (Fig. 3a) and radial (Fig. 3c) directions can be seen. In other species, peaks in the tangential (X) direction are missing (Fig. 3a). Another interesting observation in chestnut is that the majority of the oil penetrated into the wood, only minor quantities of oil remaining on the surface, which can also be seen in Fig. 6a.

In parallel to the distribution of the oil, a 3D MRM image was added for better visualisation of the tung oil distribution and penetration into the specimen (Fig. 6). MR imaging revealed not only the oil distribution but also the early-wood and late-wood areas. The 3D MRM image showed oil penetration, which was slightly higher in less dense early-wood and lower in denser late-wood. It is believed that there are simple physical phenomena behind this, since there are fewer voids available in late- than in early-wood at softwoods, hence the wooden tissue with bigger cell lumina looks better treated. Vessels in sweet chestnut (Fig. 6a) can be seen through entire specimens. No signal was detected on the surface of sweet chestnut. It can be seen that there is almost no oil on the surface, while it can be observed in the first cells below it. It seems that the oil disappeared (it was wiped off with a paper towel) or penetrated deeper into the samples. In larch samples, the majority of the tung oil remained on the surface of the specimens and the remainder penetrated into the early-wood predominantly in the longitudinal direction (Fig. 6b), which was observed on specimens situated at the edges of the original larch sample (approximately 3 mm). There were also some areas on the surface without oil. We

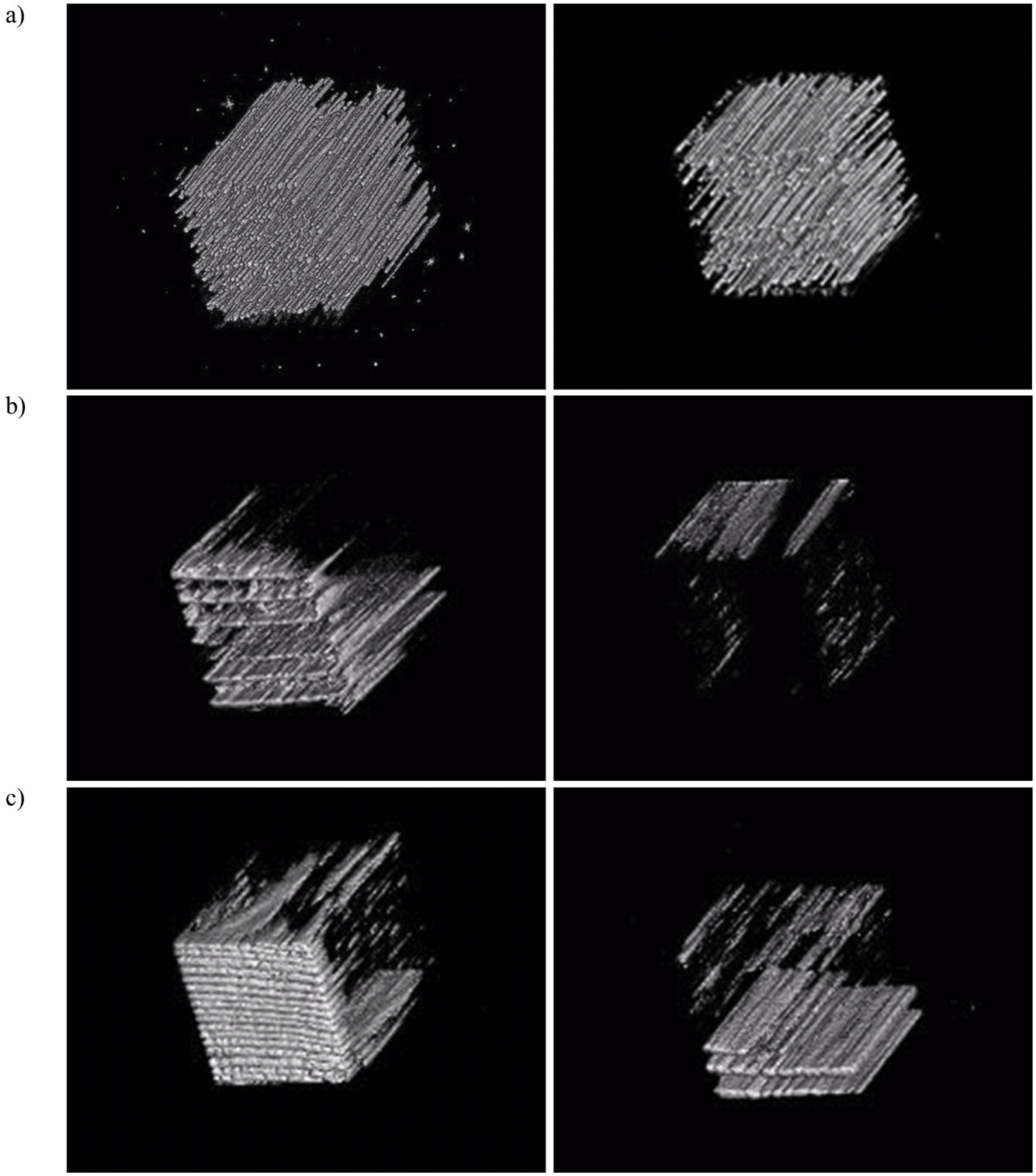

Fig. 6. MRI of Cs (a), Ld (b) and Pa (c) after vacuum-pressure impregnation. FOV was 20 mm, imaging matrix of the first column (specimen a.0) was 256 × 256 × 256 (isotropic resolution 78 μm, with total imaging time 7.5 h) and for the second column (specimen a.2) was 128 × 128 × 128 (isotropic resolution 156 μm, with total imaging time 34 min). The materials abbreviations are the same as in Table 1.

presume that the reason for this is layer of non-permeable heartwood on the surface. The remaining concentration was too low to be visible on the MR image. Macroscopic observation confirmed that these were late-wood areas on the surface. The MR image indicated that oil remained on the surface, since the larch is too refractory, having most of the pits aspirated for deeper penetration and it left inner parts of specimens less impregnated as can be seen from the MRI spectra. The most variable distribution was measured at spruce wood (Fig. 6c), in which the tung oil penetrated into the border between early and late-wood areas over the whole sample in the lower two growth rings. This pattern was notable at all of the specimens from the same group of the spruce wood specimens. Up to our best knowledge, we were not able to identify the reasons for this occurrence. Similarly as reported at sweet chestnut wood,

the axial surface of spruce wood was not fully covered with tung oil. It seems like that the oil from the surface penetrated into the inner part of the specimens after impregnation. The oil has sufficient viscosity that enables slow penetration to wood likely due to the capillary based mechanisms.

There are various techniques available for determination of the oil distribution in the wood. The most simple are gravimetric techniques. In general, the simple gravimetric approach provides information about the amount of the retained oil. However, this information does not provide any additional information regarding the distribution of oil in wood. On the other hand, tensiometer provides us more information. From this analysis, dynamics of the oil penetration into the axial (or any other planes) can be monitored. However, this technique is not (or hardly) applicable for pressure treatments. However, in order to resolve the distribution of oil in wood, there are several techniques available. One of the first imaging technique was application of ESEM (Rosenqvist, 2000). Prior to the development of the ESEM analysis of oil treated wood was avoided due to potential contamination of SEM with oil vapours. ESEM is nowadays generally available technique. However, the information provided is two dimensional, with huge influence of sample preparation similarly as reported for CLSM (Confocal Laser Scanning Microscopy)(Singh et al., 2013). Besides SEM and CLSM there were some other techniques available as well. In general, all these techniques are more challenging, longer lasting and more expensive than gravimetric techniques. For example MRM imagining of single specimen can take up to 7.5 h. Similarly is reported for other imaging techniques, like micro CT (Moghaddam et al., 2016). However, the advantage of the MRM is that recording of the two dimensional information is much faster and enables us monitoring of the processes, like wood drying or wetting in situ.

4. Conclusion

Tung oil can penetrate into wood specimens. Oil uptake depends on the applied impregnation method and on the wood species used. Retention of tung oil was higher after an impregnation process than with the immersion procedure. Longitudinal uptake of oil determined with a tensiometer was the highest with spruce wood specimens and the lowest with larch heartwood ones. To obtain the oil distribution along all three axes, 1D MRI was successfully used. The strength of MR microscopy lies in the qualitative data on oil distribution in wood. Additionally, the MRI signals are correlating nicely with uptake from impregnation and immersion processes. If the signal intensity was high enough, the MR imaging revealed not only the intensity of the signal in different parts of specimens but also the shape of the specimens. The latter was obtained with 3D MRM, which was performed by a gradient-echo technique. This technique was shown to be a suitable method for 3D visualization of the spatial oil distribution and penetration. When comparing MRM with different spatial resolutions, more information can be obtained from images with higher resolution but they are more time consuming. The data showed that pine sapwood took up the highest amounts of tung oil after vacuum-pressure impregnation. Its MRI signal was relatively uniform through the entire sample structure. In less permeable specimens, the majority of tung oil remained on the surface or penetrated only in the longitudinal direction. In the radial direction, clearly visible peaks may be associated with early and late-wood areas. In the future, we tend to use this technique to determine the oil penetration in the specimens that were after impregnation exposed to weathering and/or fungal decay. This will enable us to see if oil remains in wood or if it is degraded or leached out.

Acknowledgment

The authors acknowledge the support of the Slovenian Research Agency within the framework of project L4-5517, L4-7547, programme P4-0015.

References

Žlahtič, M., Humar, M., 2016. Influence of artificial and natural weathering on the hydrophobicity and surface properties of wood. BioResources 11 (2), 4964–4989.
Anonymous, 2016. Minor oil crops. . . http://www.fao.org/docrep/X5043E/x5043E0e.htm. (Accessed 3 March 2016).
Banks, W.B., 1970. Some factors affecting the permeability of Scots pine and Norway spruce. J. Inst. Wood Sci. 5 (1), 10–17.
Bucur, V., 2003a. Nondestructive Characterization and Imaging of Wood. Springer, Berlin, Heidelberg, New York.
Bucur, V., 2003b. Techniques for high resolution imaging of wood structure: a review. Meas. Sci. Technol. 14, R91–R98.
Comstock, G.L., 1970. Directional permeability of softwoods. Wood Fiber Sci. 1 (4), 283–289.
De Vetter, L., Van den Bulcke, J., De Windt, I., Stevens, M., Van Acker, J., 2009. Preventive action of organosilicon treatments against disfigurement of wood under laboratory and outdoor conditions. Int. Biodeterior. Biodegrad. 63, 1093–1101.
Demeure, R., Moreaux, C., Mottet, I., Dereppe, J.M., 1994. Fast MR-imaging of porous media. Magn. Reson. Mater. Phys. Biol. Med. 2 (1), 21–28.
Durmaz, S., Yildiz, U.C., Yildiz, S., 2015. Alkaline enzyme treatment of Spruce wood to increase permeability. Bioresources 10 (3), 4403–4410.
EN 1609, 1997. Thermal insulating products for building applications – Determination of short term water absorption by partial immersion CEN (European Committee for Standardisation), Brussels, Belgium.
EN 113, 2006. Wood preservatives – Test method for determining the protective effectiveness against wood-destroying basidiomycetes. Determination of toxic values. European Committee for Standardisation, Brussels, Belgium.
EN 335, 2013. Durability of wood and wood-based products – Use classes: Definitions, application to solid wood and wood-based panels. European Committee for Standardisation, Brussels, Belgium.
EN 350, 2015. Durability of wood and wood-based products – Testing and classification of the resistance to biological agents, the permeability to water and the performance of wood and wood-based materials. European Committee for Standardization, Brussels, Belgium.
Flynn, K.A., 1995. A review of the permeability, fluid-flow, and anatomy of spruce (*Picea* spp.). Wood Fiber Sci. 27 (3), 278–284.
Goethals, P., Stevens, M., 1994. Dimensional Stability and Decay Resistance of Wood upon Modification with Some New Type Chemical Reactants (IRG/WP 94-40028). International Research Group on Wood Preservation, Stockholm Sweden.
Humar, M., Lesar, B., 2013. Efficacy of linseed- and tung-oil-treated wood against wood-decay fungi and water uptake. Int. Biodeterior. Biodegrad. 85, 223–227.
Kumar, S., Morrell, J.J., 1989. Penetration and absorption of different CCA compositions in six western conifers. For. Prod. J. 39 (10), 19–24.
Lande, S., Høibø, O.A., Larnøy, E., 2010. Variation in treatability of Scots pine (Pinus sylvestris) by the chemical modification agent furfuryl alcohol dissolved in water. Wood Sci. Technol. 44, 105–118.
Larnøy, E., Lande, S., Vestøl, G., 2008. Variations of Furfuryl Alcohol and Wolmanit CX-8 Treatability of Pine Sapwood Within and Between Trees. The International Research Group on Wood Protection Document, NO IRG/WP/08-40421.
Lesar, B., Humar, M., 2010. Service life prediction of wood treated with wax emulsions and copper amine based solutions exposed in third use class. Zbornik Gozdarstva Lesarstva 93, 23–35.
Lesar, B., Humar, M., 2011. Use of wax emulsions for improvement of wood durability and sorption properties. Eur. J. Wood Prod. 69, 231–238.
Maschek, D., Goodell, B., Jellison, J., Lessard, M., Militz, H., 2013. A new approach for the study of the chemical composition of bordered pit membranes: 4Pi and confocal laser scanning microscopy. Am. J. Bot. 100, 1751–1756.
Merela, M., Sepe, A., Oven, P., Serša, I., 2005. Three-dimensional in vivo magnetic resonance microscopy of beech (*Fagus sylvatica* L.) wood. Magn. Reson. Mater. Phys. Biol. Med. 18, 171–174.
Militz, H., 1993. Enzymatic pretreatment of spruce posts and sawn boards to improve their treatability with wood preservatives. Holz Roh Werkst. 51, 339–346.
Moghaddam, M.S., Van den Bulcke, J., Wålinder, M.E.P., Claesson, P.M., Van Acker, J., Swerin, A., 2016. Microstructure of chemically modified wood using X-ray computed tomography in relation to wetting properties. Holzforschung, http://dx.doi.org/10.1515/hf-2015-0227, in press.
Moreaux, C., Dereppe, J.M., 1994. ^{23}Na microimaging of water phase in porous limestone. Magn. Reson. Mater. Phys. Biol. Med. 2 (2), 109–111.
Oven, P., Merela, M., Mikac, U., Serša, I., 2011. Application of 3D magnetic resonance microscopy to the anatomy of woody tissues. IAWA J. 32 (4), 401–414.
Palanti, S., Feci, E., Torniai, A.M., 2011. Comparison based on field tests of three low-environmental-impact wood treatments. Int. Biodeterior. Biodegrad. 65, 547–552.

Rosenqvist, M., 2000. The Distribution of Introduced Acetyl Groups and a Linseed Oil Model Substance in Wood Examined by Microautoradiography and ESEM. The International Research Group on Wood Protection, Stockholm, pp. 21, IRG/WP 00-40169.
Schultz, T.P., Darrel, D.N., Ingram, L.L., 2007. Laboratory and outdoor water repellency and dimensional stability of southern pine sapwood treated with waterborne water repellent made from resin acids. Holzforschung 61, 317–322.
Sedighi-Gilani, M., Griffa, M., Mannes, D., Lehmann, E., Carmeliet, J., Derome, D., 2012. Visualization and quantification of liquid water transport in softwood by means of neutron radiography. Int. J. Heat Mass Transf. 55, 6211–6221.
Siau, J.F., 1984. Transport Processes in Wood. Springer-Verlag, Heidelberg, pp. 245.
Singh, A.P., Park, B.-D., Nuryawan, A., Kazayawoko, M., 2013. Advances in probing wood-Coating interface by microscopy: a review. J. Surf. Eng. Mater. Adv. Technol. 3, 49–54.
Stamm, A.J., 1947. Passage of Liquids, Vapors and Dissolved Materials Through Softwoods. Technical bulletin, US Forest Products Laboratory, pp. 929.
Thybring, E.E., 2013. The decay resistance of modified wood influenced by moisture exclusion and swelling reduction. Int. Biodeterior. Biodegrad. 82, 87–95.
Wagenführ, R., 1996. Holzatlas. Fachbuchverlag, Leipzig, pp. 688.
Williams, R.S., Feist, W.C., 1999. Water Repellents and Water-repellent Preservatives for Wood. Gen. Tech. Rep. FPL-GTR-109. US Department of Agriculture. Forest Service. Forest Products Laboratory, Madison, WI.
Zimmer, K., Treu, A., McCulloh, K.A., 2014. Anatomical differences in the structural elements of fluid passage of scots pine sapwood with contrasting treatability. Wood Sci. Technol. 48, 435–447.